

Current contacts and the breakdown of the quantum Hall effect

P. C. van Son, G. H. Kruithof, and T. M. Klapwijk

*Department of Applied Physics, Materials Science Centre, University of Groningen, Nijenborgh 18,
NL-9747 AG Groningen, The Netherlands*

(Received 14 June 1990)

The nonlinearities in the IV characteristics have been studied of high-mobility Si metal oxide semiconductor field-effect transistors in the quantum Hall regime. The breakdown curves were measured with different sets of voltage contacts and for different directions of magnetic field and current. Comparison of these curves shows that the breakdown of the quantum Hall effect (QHE) in these samples is an intrinsic effect that starts at the current contact where the electrons are injected into the two-dimensional electron gas (2DEG). This fundamental asymmetry and the crucial role of the current contact are explained using the Büttiker-Landauer approach to the QHE and its recent extension to the nonlinear regime. The electron-injection process contains two mechanisms that lead to breakdown voltages in the 2DEG. We have identified both experimentally by comparing the critical currents of different configurations of current and voltage contacts. In one of the mechanisms, the nonequilibrium distribution of electrons that is injected into the 2DEG extends to the voltage contacts. This means that the equilibration length of the 2D electrons is at least of the order of $100\ \mu\text{m}$. For currents far beyond breakdown and for voltage contacts that are further from the electron-injection contact, the breakdown characteristics are harder to understand. The variation of the electron density of the 2DEG due to the large Hall voltage has to be taken into account as well as the equilibration induced by additional voltage contacts.

I. INTRODUCTION

The understanding of the quantum Hall effect (QHE) still evolves as more experimental results become available. Existing models of the QHE are extended or new models are developed to explain new aspects of the high-field magnetotransport of the two-dimensional electron gas (2DEG). Several approaches have been reviewed by Prange and Girvin¹ together with the basic experimental facts about the QHE. These models generally treat the QHE as a bulk 2D effect and do not explicitly consider the edges of the sample nor the current and voltage contacts that are used in an actual measurement. Recently, Büttiker² sketched a new approach to the QHE in which these aspects are taken into account. The electrons occupying the quantum-mechanical edge states³⁻⁵ of the sample play a crucial role. Electrons on opposite edges of the sample carry current in opposite directions. A net current is obtained if the current contacts fill the edge states up to different values of the electrochemical potential. Voltage contacts only couple to the electron states of their own edge. The QHE occurs if there is no (back)scattering from one edge to the other. This is argued to occur when in the bulk the electron states at the Fermi level are localized. With the assumption of localized states Büttiker's approach connects with the earlier models of the QHE. His approach has already been successfully applied to 2DEG samples in the QH regime that contain an adjustable barrier.⁶

In the QH regime, the Hall resistance of the 2DEG is given by $h/(ie^2)$ with integer i , the number of occupied electron levels (two or four per Landau level). At the same time the longitudinal resistance, measured between

voltage contacts on the same edge, vanishes. It was first shown by Ebert *et al.*⁷ and by Cage *et al.*⁸ that the zero-resistance state disappears if the current is increased beyond a critical value. This so-called breakdown of the QHE and the value of the critical current are experimental observations that need to be understood in the context of a complete model of the QHE. Although several mechanisms for breakdown have been proposed, a complete picture has not yet emerged. The reason is that sample inhomogeneities often play an important role, and that the geometry of sample and contacts is sometimes neglected: The relevant breakdown mechanism may be different for different experimental geometries. In this paper we study the recently discovered influence of the current contacts on the breakdown of the QHE in a common Hall bar.⁹ We show that our results can be understood in terms of nonequilibrium occupations of the edge states near the electron-injection contact. A breakdown voltage is measured when this nonequilibrium is detected by the voltage contacts. Specifically, we show that we observe experimentally the two breakdown mechanisms contained in the model of the electron-injection process.¹⁰ First, however, we give a brief review of experiments on and theories of the breakdown of the QHE.

The breakdown of the QHE has been measured mostly in (Hall) bars but also in the Corbino geometry¹¹ and in the van der Pauw geometry.¹² In a Corbino disc one measures the conductivity, which is zero in the QH regime and increases when the voltage across the inner and outer contact exceeds a critical value. This seems very different from the above-described breakdown in a Hall bar where the (four-terminal) resistance deviates from zero beyond a critical current. However, both phenome-

na can be described with the appearance of a (dissipative) current component in the direction of the voltage. The breakdown current and voltage are related to each other through the Hall resistance (as are the current density at breakdown and the electric field). Proposed breakdown mechanisms usually apply both to Corbino discs and to Hall bars. An obvious exception is the influence of the current contacts of a Hall bar on the breakdown of the QHE, which is the subject of this paper. In the following we will restrict ourselves to samples with the Hall-bar geometry.

The first breakdown measurements were done on ordinary (wide) Hall bars.^{7,8,13–15} Later, constrictions were applied to the 2DEG to study the breakdown in a well-defined (narrow) part of the sample^{16–19} and breakdown measurements were done on completely submicrometer Hall bars.²⁰ Depending on the geometry breakdown may first occur in the bulk or at the edges. The critical current is either proportional to the width (bulk breakdown) or independent of it (edge breakdown). In the latter case there may be an additional bulk current present^{3,10} making the total critical current depend again on the width of the sample. Kirtley *et al.*¹⁶ have proposed an edge-current model to describe their breakdown results on constrictions with widths of the order of 1 μm . In their model, breakdown occurs when the Hall voltage equals the Landau-level separation. Most other theoretical approaches, however, are bulk models which yield a critical (Hall) electric field for breakdown.

For breakdown in the bulk, four mechanisms have been proposed. The first is a heating instability.^{7,14} With increasing current, the resistivity of the 2DEG increases and therewith the dissipation. At the critical current the dissipated power increases faster than the heat transfer from the electron gas to the phonon system. The electron temperature suddenly rises and the QHE disappears. A second more microscopic model features the Cerenkov emission of phonons.²¹ Because of conservation of energy and momentum, electrons in a single Landau level can only emit phonons when their drift velocity exceeds the speed of sound (intra-Landau-level scattering). This yields a critical electric field for the occurrence of dissipation because the drift velocity is proportional to the electric field. In the third model, tunneling of the electrons to the lowest unoccupied Landau level is considered (inter-Landau-level scattering). At a critical electric field the wave functions at the same energy in different Landau levels overlap and tunneling is possible.²² The momentum change of the electron is absorbed in the emission of a phonon (quasi-elastic^{23,24}) or by an impurity.²⁵ Finally Trugman^{26,27} considered the potential fluctuations in the 2DEG that cause the localized states that appear in most models of the QHE. If the potential fluctuations are smooth, the electric (Hall) field causes the delocalization of the electrons and therewith the breakdown of the QHE.²⁶ For abrupt potential fluctuations an analysis of the scattering dynamics yields a transverse displacement if the electron velocity exceeds a critical value.²⁷ This means that at a critical current density a dissipative current component appears in the sample.

Experimentally, the relevant breakdown mechanism is

hard to identify. The most important reason is that the current distribution in the sample is not known. Edge currents play a role and in the bulk the current distribution may be highly inhomogeneous even for small sample inhomogeneities.¹ This explains the large spread in the measured critical current densities. Two additional experimental observations have hardly been considered yet theoretically. The first is the dependence of the critical current on the filling of the Landau levels. Mostly a triangular dependence is found with the maximum critical current at integer filling factor.^{7,16,17,20} Secondly, beyond the critical current, switching among distinct dissipative states has been observed.^{8,28,29}

An experimental feature that has obtained more attention is the structure in the breakdown curves beyond the critical current. For narrow constrictions this structure has been related to the Landau levels,¹⁶ to resonant reflection between the edge states,⁵ to inhomogeneities,¹⁹ and to coherent inter-Landau-level scattering.^{17,24} The latter effect has also been used to explain the structure observed in wide Hall bars.²⁹ However, for wide samples the structure is usually ascribed to the successive breakdown of localized parts of the (inhomogeneous) sample. This seems to be supported by the observation that the critical current and the breakdown structure differ when measured between different voltage contacts on the same sample. However, in some experiments on wide Hall bars^{9,28} it is shown that the structure reproduces between opposite voltage contacts if also the directions of magnetic field and current are reversed. This clearly shows that here the breakdown structure has an intrinsic origin and is not due to inhomogeneities.

Mokerov *et al.*²⁸ concluded that the direction of the Hall field is the relevant parameter for the intrinsic breakdown structure and that the current contacts have no influence. However, van Son *et al.*⁹ showed that in their geometry an intrinsic sequence occurs in which the current contacts play a crucial role. The breakdown starts in the corner where the electrons are injected into the 2DEG and spreads from there through the whole sample to the other current contact. Indications for the special role of the current contacts in the breakdown of the QHE were found before by Yoshihiro *et al.*¹⁵ This role is not surprising, as in the QH regime the dissipation occurs in and near the current contacts. The asymmetric behavior of the current source and sink, however, cannot be explained in a macroscopic heating model. Büttiker's model of the QHE contains a microscopic description of the current contacts, but in his approach current source and sink still behave symmetrically. Recently, Büttiker's model has been extended into the nonlinear regime¹⁰ and then it shows the asymmetry that is also observed experimentally.

In this paper we illustrate the role of the current contacts in the breakdown of the QHE in homogeneous Si metal oxide semiconductor field-effect transistors (MOSFET's) with a Hall-bar geometry, and we connect the measurements to the extended Büttiker model. In Sec. II we discuss the model with an emphasis on the nonequilibrium effects near the electron-injection contact. Sample characteristics and the experimental setup are de-

scribed in Sec. III. In Sec. IV we discuss our results and show that the two breakdown mechanisms contained in the model are observed experimentally. Our conclusions are summarized in Sec. V.

II. ELECTRON-INJECTION CONTACT IN THE QUANTUM HALL REGIME

In his description of the QHE, Büttiker² deals explicitly with open multiprobe conductors such as Hall bars. The contacts are equilibrium reservoirs of electrons with a well-defined electrochemical potential. The electron states in the sample are occupied through the interaction with the contacts, not necessarily leading to an equilibrium distribution. The local electrochemical potential in the sample is therefore not always defined. The potentials of the current contacts are set and maintained externally, while the potentials of the voltage contacts are determined self-consistently through the demand that the contacts draw no net current. These concepts have been developed by Landauer³⁰ for the description of electrical conduction in one dimension. They apply well to the QHE because the high magnetic field absorbs one degree of freedom of the two-dimensional electron gas by creating Landau levels. The electrons in a Landau level essentially form a one-dimensional conducting channel. If more than one Landau level is occupied, multichannel generalizations of Landauer's formula³¹ can be applied.

For current transport in the QH regime the quantum-mechanical edge states are very important.³⁻⁵ In the bulk the Fermi level lies in the localized states which do not carry current. Due to the confining potential, the Landau-level energy rises at the edges of the sample and crosses the Fermi level. Classically these edge states correspond to skipping orbits and they are the only extended states at the Fermi level. In the linear regime (applied voltages much smaller than the Landau-level separation) these are the only relevant states for the determination of the transport properties. The electrons on opposite edges move in opposite directions. A net current flows through the sample if the edge states are occupied up to different energy levels. Büttiker² showed that the QHE is obtained if the electrons in the edge states obey a thermal equilibrium distribution and if they cannot scatter into states on the opposite edge (absence of backscattering). The quantization of the Hall resistance to $h/(ie^2)$ with integer i is due to the fact that the density of states and the group velocity of the electrons compensate each other in the expression for the conductivity of a one-dimensional conductor.^{30,3,2,31} The voltage difference between voltage contacts on the same edge is zero because the occupation of the edge states is constant as long as there is no backscattering. Even with a moderate amount of scattering centers present in the sample, backscattering is suppressed in the QH regime because the electron states that carry current in opposite directions are spatially well separated.²

Büttiker² discusses explicitly the interaction of the current and voltage contacts with the edge states of the QH sample. Ideal contacts absorb all electrons in incoming edge states irrespective of their energy. The contacts

feed all outgoing edge states with an equilibrium distribution of electrons that corresponds to the electrochemical potential of the contact. Nonideal contacts reflect some of the incoming electrons elastically into outgoing states and do not fill all available outgoing edge states. For such contacts the QHE is established only after relaxation of the nonequilibrium distribution through inelastic scattering. The current contacts supply a net current to the sample, while the voltage contacts acquire an electrochemical potential such that incoming and outgoing edge currents cancel. Note that an ideal (voltage) contact transforms a nonequilibrium distribution of incoming electrons into an equilibrium outgoing distribution and that is thus helps in establishing the QHE. These concepts have been applied successfully to several experiments.⁶ Nonequilibrium occupations of edge states were created with gates on the sample or with quantum point contacts while the effects were detected with (nonideal) voltage contacts or again quantum point contacts. All these experiments were done in the linear regime (small applied voltage) where Büttiker's model is directly applicable.

Recently, larger applied voltages have also been considered with the Büttiker approach.¹⁰ Due to the (Hall) electric field the electrons in extended states in the bulk acquire a drift velocity and participate in the current. If the field is not too large, backscattering and scattering into unoccupied Landau levels are still absent and Büttiker's model for the most part applies. Only the electron-injection process is more complicated because the supply of the bulk current also has to be considered. Beyond a critical current value the injecting contact supplies a nonequilibrium distribution of electrons to the 2DEG, even if it is an ideal contact for small currents. If the nonequilibrium distribution does not relax before it reaches the voltage contacts, deviations from the QHE (breakdown) are to be expected analogous to what happens in a sample with nonideal contacts. We will demonstrate that two breakdown mechanisms result from the electron-injection process and that they manifest themselves at the two edges of the sample, respectively.

Figure 1 shows schematically the current distribution in a Hall-bar sample and the energy level of the electrons.¹⁰ The slope of the levels in the bulk is due to the (Hall) electric field, and the almost vertical sections correspond to the edge states. Far from the electron-injection contact the levels will be filled as indicated in Fig. 1(b). In the bulk the Fermi level lies in between two Landau levels and the edge states are filled up to μ_1 and μ_2 , respectively. This situation corresponds to a quantized Hall resistance and to zero longitudinal resistance. In the current contacts the Hall field is negligible, therefore near the contacts the electrostatic potential in the 2DEG has to adapt itself as indicated in Fig. 1(c). The electrons in extended states in the 2DEG move along equipotentials with a velocity that is proportional to the slope of the energy level.³ Three types of trajectories have been indicated in Fig. 1(c). The μ_1 -edge states (trajectory 1) are filled by the right-hand-side current contact. The electrons interact with the voltage contact and are finally absorbed by the μ_2 current-contact. The μ_2 -edge states are filled by

the right-hand-side current contact. The electrons cannot enter the μ_1 current contact because of the increasing electrostatic potential. Instead, they move along equipotentials to bulk states in which they return to the μ_2 current contact. Because of the cancellation of group velocity and density of states, all bulk states up to μ_2 are filled in this way. Trajectories of type (2) are similar to those of type (3) except that they are not filled by the μ_2 current contact. They have to be filled by the μ_1 current contact, which requires tunnel transitions or inelastic scattering of electrons originally injected at higher energies. This situation only exists if $\mu_2 < \mu'_1$, which for integer filling factor is equivalent to $(\mu_1 - \mu_2) > \hbar\omega_c/2$ ($\hbar\omega_c$ is the Landau-level separation). As soon as trajectories of type (2) are present, a nonequilibrium distribution of electrons is injected into the 2DEG. In contrast, the μ_2 current contact simply absorbs all electrons moving towards it (if it is an ideal contact) and here no nonequilibrium electron distribution is injected into the 2DEG. This yields an asymmetric behavior of the two current contacts. In the following we concentrate on the electron-injection contact.

There are two ways in which a nonequilibrium electron distribution gives rise to voltage differences that are not present in the QHE (see Fig. 2). We first consider the μ_1 edge. Along the width of the current contact, electrons

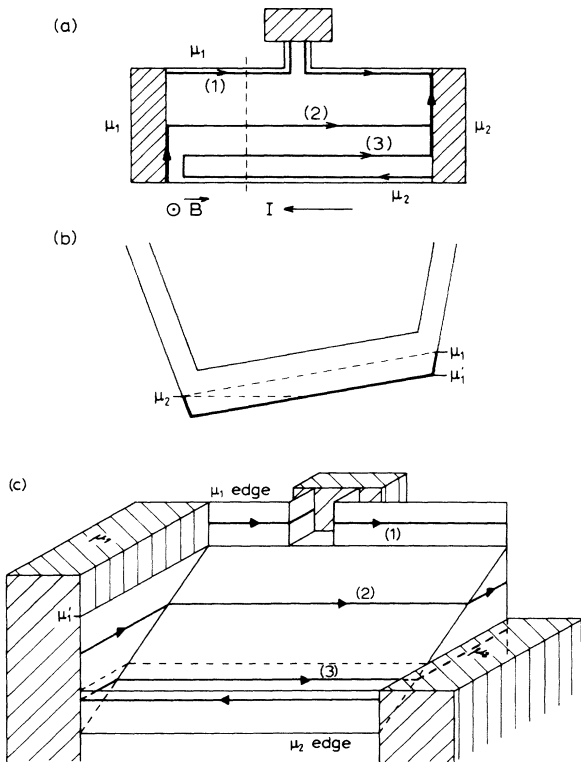


FIG. 1. Current distribution (a) and energy levels of the electrons (b) and (c) in the Hall-bar sample with two current contacts and one voltage contact. (b) is a cross section along the dashed line shown in (a), while (c) provides a perspective view of the highest occupied Landau level. Three types of electron trajectories have been indicated in (a) and (c).

are injected at the μ'_1 level and scatter inelastically into the empty states at lower energies. If the contact is wide enough, all electron states up to μ'_1 will be filled in this way and at the μ_1 edge an equilibrium electron distribution with electrochemical potential μ_1 is established (all edge states between μ'_1 and μ_1 are filled directly by the current contact). However, if the contact is narrower, some states remain empty up to the μ_1 edge and electrons from the μ_1 -edge states will scatter into them. Then a voltage difference develops between the voltage contact on the μ_1 edge and the μ_1 current contact (breakdown). Next we consider the μ_2 edge. Because of the large potential gradient near the current contact, electrons can tunnel there to empty states in the 2DEG. Especially in the energy interval between μ'_1 and μ_1 , electrons can tunnel from the contact to the higher (normally unoccupied) Landau level of Fig. 2(a). These electrons will scatter eventually into the lower Landau level. Until that happens, they drift through the bulk towards the μ_2 current contact but also scatter into the empty edge states of the μ_2 edge [Fig. 2(b), note that in this nonequilibrium situation backscattering is not impossible]. If the occupation of the higher Landau level extends beyond the first voltage contact on the μ_2 edge, the additional electrons in the edge states give rise to a voltage difference between that contact and the next voltage contact on the μ_2 edge (breakdown).

In the model of the electron-injection process there is a threshold for the injection of a nonequilibrium electron distribution into the 2DEG. However, the critical value of the current for the observation of breakdown at the

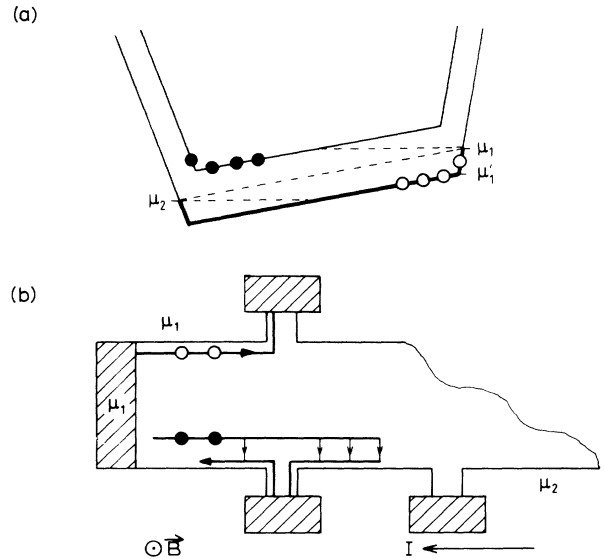


FIG. 2. Nonequilibrium occupancies of the current-carrying states near the electron-injecting contact showing the two breakdown mechanisms. On the high-energy (μ_1) edge the incomplete filling of the lower Landau level leads to a (breakdown) voltage difference between current and voltage contact. On the low-energy (μ_2) edge the nonequilibrium occupancy of the higher Landau level gives rise to a (breakdown) voltage difference between the two voltage contacts on that edge.

contacts will be larger than that threshold. It will depend for instance on the inelastic scattering time of the electrons and also on the geometry of the current and voltage contacts. The breakdown at the high-energy edge of the sample (μ_1 edge) is related to the fact that electron states in the highest occupied Landau level remain empty. The associated critical current will therefore scale with the width of the injecting contact. The breakdown at the low-energy edge (μ_2 edge) corresponds to the occupation of electron states in the lowest normally unoccupied Landau level. Here the width of the current contact is not important. Because of the finite equilibration length of the electrons, the critical current will depend on the separation of the electron-injection contact and the nearest of the two voltage contacts employed. These geometrical considerations have been used to identify the two breakdown mechanisms experimentally.

III. SAMPLE CHARACTERISTICS AND EXPERIMENTAL SETUP

The measurements were performed on Si MOSFET's with peak mobilities of $2-3 \text{ m}^2/\text{Vs}$. The standard thickness of the gate oxide was 100 nm, but one series (sample 3) was produced with a 200-nm gate oxide. More detailed information about these samples is given in Ref. 32. The geometry and the relevant dimensions of the 2DEG and the contacts are shown in Fig. 3. The contacts were made by ion implantation of phosphorous and a subsequent diffusion. The contact resistances (measured in a three-terminal configuration in the QH regime) ranged from less than 10 to 100 Ω . In the breakdown characteristics no influence was observed of these different contact resistances. One series of MOSFET's (sample 1) was produced in which the 2DEG is only 180 μm wide and does not overlap the contacts 1-3 (see Fig. 3).

All measurements were performed in a magnetic field $B = 12 \text{ T}$ with the sample immersed in a pumped He bath ($T = 1.1 \text{ K}$). For the breakdown measurements, the gate voltage was adjusted to obtain a filling factor $i = 4$ (first Landau level completely filled). This gate voltage is not too far from the value where the mobility shows its max-

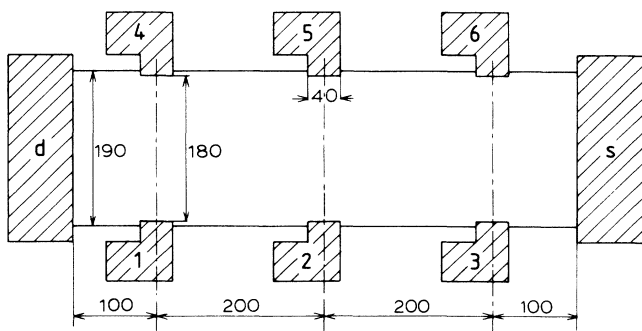


FIG. 3. Geometry of the 2DEG and the surrounding n^+ -implanted areas (hatched boxes) that act as current and voltage contacts (all dimensions are in micrometers). In sample 1 the 2DEG is only 180 μm wide and positioned such that contacts 1-3 are disconnected.

imum. A home-built current source supplied a direct current to the sample and a small ac modulation (83 Hz, 100 nA). The current source operated symmetrically, i.e., the midpoint of the sample was kept at a fixed voltage with respect to the gate. The direct current between contacts i and j was increased in steps and each time the differential resistance $R_{ij,kl}$ between the voltage contacts k and l was measured with a lock-in amplifier. In the same setup, measurements were done for fixed (zero) direct current but varying the gate voltage.

IV. RESULTS AND DISCUSSION

Before we discuss the breakdown characteristics of our Si MOSFET's, we first show in Fig. 4 the longitudinal resistance $R_{ds,12}$ as a function of gate voltage V_g . The fully developed minima at $V_g = 5.8$ and 8.45 V correspond to complete fillings of the first Landau level ($i = 4$) and of the lowest spin band of the second Landau level ($i = 6$), respectively. The minima due to valley splitting do not completely reach zero resistance at the available magnetic field and temperature. In the same figure we show the effect of the superposition of direct currents I_{dc} of 70 μA and of 300 μA . Already the first value is larger than the maximum current used in the breakdown characteristics that we will discuss below. The differential resistance curve is very complicated but it is still dominated by the Landau-level structure. This justifies the attempt to explain the breakdown process in terms of nonequilibrium occupations of Landau levels instead of simple electron heating. Only at $I_{dc} = 300 \mu\text{A}$ does the differential resistance curve show the expected shape for an elevated electron temperature.

Figure 5 shows typical breakdown characteristics for a standard sample (2) at the $i = 4$ QH plateau.⁹ For zero direct current from drain to source the differential resistances between voltage contacts on the same edge are zero. The critical current beyond which resistance appears depends on the positions of the voltage contacts

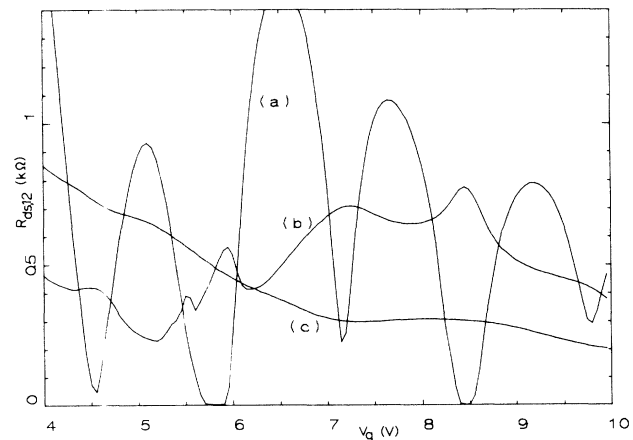


FIG. 4. Differential resistance $R_{ds,12}$ as a function of gate voltage showing how the Shubnikov-de Haas oscillations disappear as the value of the direct current is increased (sample 2, $B = 12 \text{ T}$, $T = 1.1 \text{ K}$). Curve (a) $I_{dc} = 0$, curve (b) $I_{dc} = 70 \mu\text{A}$, curve (c) $I_{dc} = 300 \mu\text{A}$.

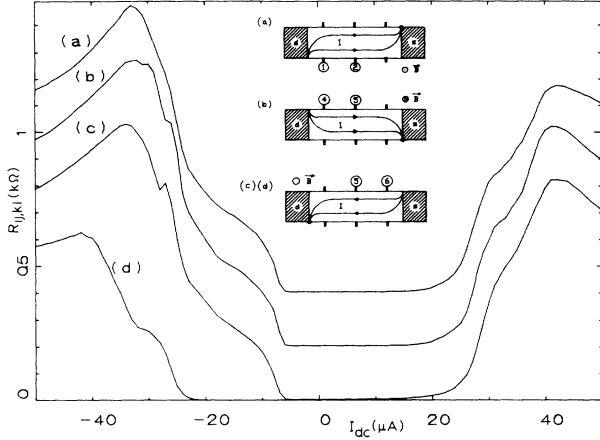


FIG. 5. Differential resistance as a function of direct current of a standard Si MOSFET (sample 2) at the $i=4$ QH plateau ($B=12$ T, $T=1.1$ K). The curves correspond to different configurations of contacts and to different directions of magnetic field and positive current (see the insets; the dots indicate the low-energy side of the electron-injection contact). The reproducibility of curves (a), (b), and (c) (that have been shifted for clarity) shows that the breakdown characteristics have an intrinsic origin. Curve (d) (only shown for negative I_{dc}) corresponds to the setup of curve (c), except for the use of voltage contacts 4 and 5.

and on the directions of the magnetic field and of the current. The structure and the asymmetry of the breakdown characteristics are not due to inhomogeneities in the sample. For different directions of the magnetic field and of the (positive) current, the structure reproduces between different voltage contacts [Figs. 5(a)–5(c)]. The voltage contacts are selected to have the same relative position with respect to the low-energy side of the electron-injection contact (indicated by the dots in the insets of Fig. 5). Only the small differences among these curves may be due to inhomogeneities in the 2DEG or to small asymmetries in the geometry of the sample. From this observation and from the comparison of the breakdown between different contact pairs but for the same directions of field and current [e.g., Figs. 5(c) and 5(d)] it has been concluded that the breakdown of the QHE shows an intrinsic sequence that starts at the current contact that injects the electrons into the 2DEG and spreads from there through the whole sample.⁹ The asymmetric behavior of the two current contacts again excludes an explanation in terms of the heating of the electron gas, because in such a model the dissipation is symmetric.

Our model of the electron-injection process (Sec. II) explains the observed asymmetry microscopically. It contains two mechanisms that give rise to breakdown voltages near the electron-injecting contact. The associated critical currents depend in different ways on the geometry. To test the model we therefore performed breakdown measurements with different configurations of current and voltage contacts (Figs. 6 and 7). We first consider the breakdown mechanism at the high-energy edge of the sample (μ_1 edge in Fig. 2). The breakdown voltage is measured between the current contact and the first voltage contact on that edge. In Fig. 6 results are

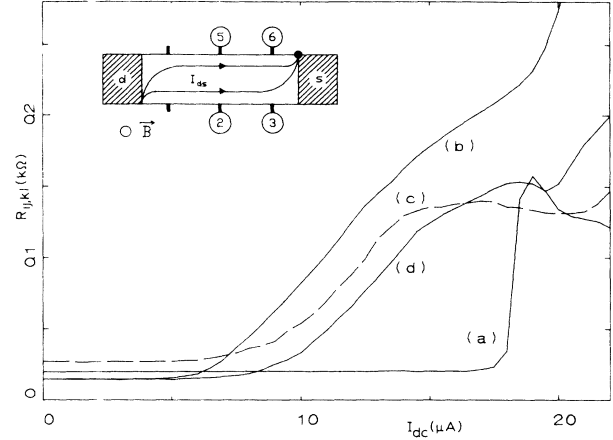


FIG. 6. Breakdown characteristics of the high-energy edge of the sample for different contact configurations (three-terminal measurements, $i=4$, $B=12$ T, $T=1.1$ K, sample 2). Curve (a) $R_{ds,3s}$ (injector: s), curve (b) $R_{d3,23}$ (injector: 3), curve (c) $R_{d6,56}$ (injector: 6), and curve (d) $R_{d5,65}$ (injector: 5). The much larger critical current in curve (a) is due to the larger width of the current contact.

shown that correspond to four different configurations in which the source contact (s) and contacts 3, 6, and 5, respectively, act as the injectors of electrons. As these are three-terminal measurements, the resistance at zero direct current is not zero but equals the contact resistance of the current contact which is higher for 6 than for 3, 5, and s . In this configuration, breakdown is due to the fact that the electron-injecting contact is not able to fill all outgoing states of the highest occupied Landau level. Clearly the critical current of the wide contact [Fig. 6(a)] is much larger than that of the narrow contacts. A different distance between the injector and the voltage contact [80 μm in Fig. 6(c) and 160 μm in Fig. 6(d)] does not change the critical current. This is not surprising, be-

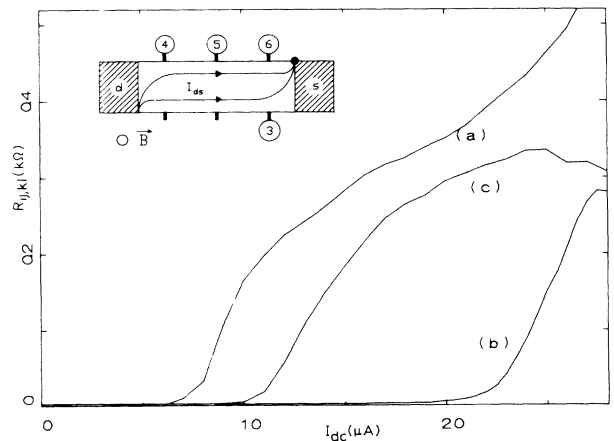


FIG. 7. Breakdown characteristics of the low-energy edge of the sample for different contact configurations ($i=4$, $B=12$ T, $T=1.1$ K, sample 2). Curve (a) $R_{ds,56}$ (injector: s), curve (b) $R_{d6,45}$ (injector: 6), and curve (c) $R_{d3,65}$ (injector: 3). The much larger critical current in curve (b) is due to the larger separation of the current and voltage contacts.

cause this voltage contact only supplies a reference while the breakdown is detected by the nearest voltage contact (which is in this case the injector itself). Note that the higher resistance of contact 6 has no influence on its breakdown behavior.

The second breakdown mechanism in our model is related to the low-energy edge of the sample (μ_2 edge in Fig. 2). Here the breakdown voltage is due to the nonequilibrium occupation of the normally unoccupied Landau level at the position of the nearest voltage contact. In Fig. 7 we compare the results of three configurations of contacts with, respectively, the source contact and contacts 6 and 3 as the injectors of electrons. Because of the equilibration length, the critical current is larger when the voltage contact is separated more from the current contact [$80 \mu\text{m}$ in Fig. 7(a) and $160 \mu\text{m}$ in Fig. 7(b)]. The critical currents in Figs. 7(a) and 7(c) are almost the same, which confirms that the width of the current contact is not important now. The slightly larger critical current in Fig. 7(c) as well as the smaller differential resistance far beyond breakdown are probably due to the geometry: In the configuration of Fig. 7(c) the electrostatic potential bends the electrons in bulk states away from the voltage contacts.

Individually, Figs. 6 and 7 confirm the two breakdown mechanisms described in Sec. II. From a comparison of these figures an additional point can be made. If the current is sent from drain to source, breakdown occurs between contacts 5 and 6 at $I_{\text{dc}} = 8 \mu\text{A}$ [Fig. 7(a)], and only at $I_{\text{dc}} = 18 \mu\text{A}$ between the source and contact 3 [Fig. 6(a)]. This means that, while a breakdown voltage appears in the sample, the two-terminal resistance (measured between source and drain) does not change. This remarkable phenomenon has a natural explanation within our model. The breakdown at the low-energy edge does not influence the two-terminal resistance directly. Because of equilibration and backscattering of the nonequilibrium electrons in the higher Landau level, the Hall voltage $(\mu_1 - \mu_2)/e$ keeps its quantized value far from the electron-injection contact. As long as the nonequilibrium electron distribution does not extend to the other current contact, this is also the voltage difference between the two current contacts. In contrast, breakdown at the high-energy edge of the sample immediately yields an increase of the voltage difference between source and drain. Because the two breakdown mechanisms are independent of each other, it is possible that in a sample with relatively wide current contacts there is a regime of direct current in which the two-terminal resistance is quantized while some voltage contacts measure deviations from the QHE.

The initial stages of the breakdown process between voltage contacts close to the electron-injection contact are described well by the model of Sec. II. However, for larger current values, breakdown occurs also between voltage contacts that are further away [Fig. 5(d)], and additional structure is observed in the breakdown characteristics of the nearby contacts. This regime is not fully understood and at present we can only make some general remarks about it. As we have already argued above, this regime should still be described in terms of nonequilibrium

distributions of electrons over the Landau levels.

We first discuss the influence of the Hall voltage on the breakdown results. Especially for large currents the Hall voltage V_H is no longer negligible compared with the gate voltage ($V_H = 0.26 \text{ V}$ for $I_{\text{dc}} = 40 \mu\text{A}$ and $i = 4$). For a MOSFET this means that the electron density varies across the width of the sample and that it can reach values at the edges for which in a normal setup the QHE has disappeared (the width of the $i = 4$ minimum in Fig. 4 is only 0.2 V). We have studied this effect using MOSFET's with a 200-nm gate oxide (sample 3). In these otherwise identical samples the numerical factor between gate voltage and electron density is different, which results in halving the influence of the Hall voltage. The breakdown characteristic is shown in Fig. 8, where we compare it with results for gate voltages differing by $\pm 0.1 \text{ V}$. For negative currents (voltage contacts close to the electron-injection contact) the curves are mutually similar and similar to Fig. 5(a) as long as the current is smaller than $25 \mu\text{A}$. This means that for the initial stages of the breakdown process the influence of the Hall voltage may be neglected. For larger currents and for positive ones this is no longer justified, which complicates the interpretation of the later stages of the breakdown sequence.

We also studied experimentally the influence of the voltage contacts on the breakdown characteristics. According to Büttiker's model the voltage contacts can be efficient sources of relaxation of the nonequilibrium electron distribution and therefore their mere presence may have influence. In Fig. 9 we show a result of a sample (1) in which the 2DEG does not overlap the voltage contacts 1–3 (see Fig. 3) and compare it to corresponding results of samples 3 and 2 [repeated from Figs. 8(a) and 7(a), respectively]. For positive currents smaller than $20 \mu\text{A}$ the breakdown characteristic of sample 1 is not significantly different from the other two. The presence of additional voltage contacts is apparently not important for the initial stages of the breakdown sequence. For negative current, however, sample 1 shows a much smaller critical

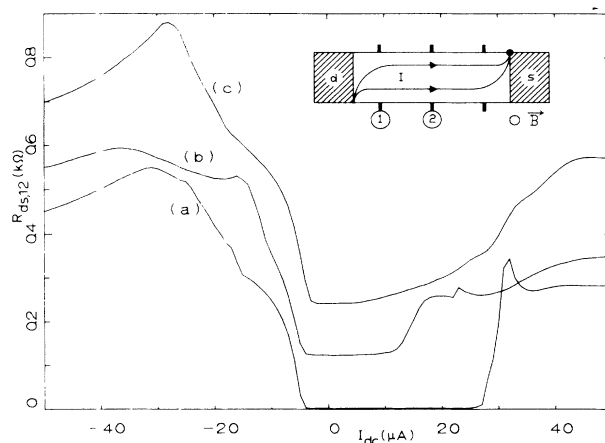


FIG. 8. Differential resistance $R_{ds,12}$ as a function of direct current for sample 3 (200-nm gate oxide, $B = 12 \text{ T}$, $T = 1.1 \text{ K}$). Curve (a) $V_g = 12.4 \text{ V}$ ($i = 4$), curve (b) $V_g = 12.3 \text{ V}$, and curve (c) $V_g = 12.5 \text{ V}$ (the latter two curves have been shifted for clarity).

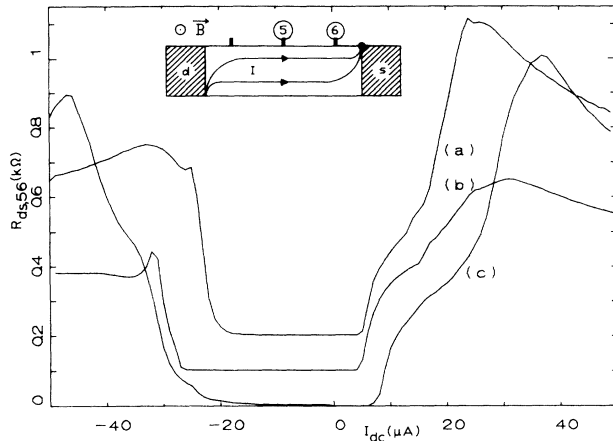


FIG. 9. Curve (a) breakdown characteristic $R_{ds,56}$ of sample 1 (missing voltage contacts 1–3). Curve (b) corresponding breakdown characteristic of sample 3 [Fig. 8(a)]. Curve (c) same of sample 2 [Fig. 7(a)].

current. In this configuration, breakdown occurs when the nonequilibrium electron distribution extends at least over half of the sample. This situation is reached for a smaller current value if some of the voltage contacts are missing. The differences between Figs. 9(a) and 9(c) for larger negative currents may also be due to the presence or absence of additional voltage contacts.

A final remark has to be made about the relaxation processes. The breakdown voltage on the low-energy edge of the sample has been successfully ascribed to a nonequilibrium distribution of electrons injected by the current contact. This means that the relaxation length in our Si MOSFET's is at least of the order of $100 \mu\text{m}$ under the given circumstances. Such surprisingly long relaxation lengths have also been found in GaAs-Al_{1-x}Ga_xAs heterojunctions with nonequilibrium populations of edge states.⁶ The vanishing overlap of the wave functions of the electrons in edge states has been proposed as an explanation of this phenomenon.³³ Apparently the relaxation length is large for electrons in bulk states as well.

V. CONCLUSION

The breakdown of the QHE that occurs when a large current is sent through the 2DEG can be used to study indirectly the QHE itself. However, also the geometry of

the sample and the homogeneity of the 2DEG determine which mechanism eventually causes the breakdown, so they have to be considered for each experiment individually. We studied the breakdown of the QHE in homogeneous Si MOSFET's with a contact geometry that allows us to observe breakdown induced by the electron-injection contact. This is concluded from the (a)symmetries that are observed in the breakdown characteristics of different voltage contacts. In the experiment two different mechanisms determine the breakdown on the two edges of the sample. They are distinguished through their different dependences on the width of the current contact and on the separation between current and voltage contacts.

We have interpreted our results using Büttiker's edge-current model of the QHE. The model has been extended to explain the asymmetric behavior of the two current contacts in the nonlinear regime. In the extended model a nonequilibrium distribution of electrons is injected into the 2DEG beyond a critical value of the current. For larger currents the nonequilibrium extends far enough into the sample to give rise to breakdown voltages close to the current contact. Different mechanisms are active on the two edges of the sample and these have been identified with the two mechanisms observed experimentally. This confirms qualitatively Büttiker's approach to the QHE and the description of the electron-injection process in the extended model. Moreover, it shows that the relaxation length of the nonequilibrium electron distribution is at least of the order of $100 \mu\text{m}$, even when both bulk and edge states are out of equilibrium. For even larger currents a nonequilibrium electron distribution is present in the whole sample. In this regime the breakdown characteristics depend among other things on the presence of additional voltage contacts because they contribute significantly to the relaxation of the electron distribution. The full shape of the breakdown characteristics and the large relaxation length of the electrons are features that remain to be explained.

ACKNOWLEDGMENTS

It is a pleasure to thank S. Bakker for the skillful preparation of the Si MOSFET's. We thank Stichting FOM for financial support. The research of Dr. van Son has been made possible by the support of the Royal Netherlands Academy of Arts and Sciences.

¹The *Quantum Hall Effect*, edited by R. E. Prange and S. M. Girvin (Springer-Verlag, New York, 1987).

²M. Büttiker, *Phys. Rev. B* **38**, 9375 (1988).

³B. I. Halperin, *Phys. Rev. B* **25**, 2185 (1982).

⁴P. Streda, J. Kucera, and A. H. MacDonald, *Phys. Rev. Lett.* **59**, 1973 (1987).

⁵J. K. Jain and S. A. Kivelson, *Phys. Rev. B* **37**, 4276 (1988); *Phys. Rev. Lett.* **60**, 1542 (1988).

⁶R. J. Haug, A. H. MacDonald, P. Streda, and K. von Klitzing, *Phys. Rev. Lett.* **61**, 2797 (1988); S. Washburn, A. B. Fowler, H. Schmid, and D. Kern, *Phys. Rev. Lett.* **61**, 2801 (1988); B.

J. van Wees, E. M. M. Willems, C. J. P. M. Harmans, C. W. J. Beenakker, H. van Houten, J. G. Williamson, C. T. Foxon, and J. J. Harris, *ibid.* **62**, 1181 (1989); S. Komiyama, H. Hirai, S. Sasa, and S. Hiyamizu, *Phys. Rev. B* **40**, 12566 (1989); B. W. Alphenaar, P. L. McEuen, R. G. Wheeler, and R. N. Sacks, *Phys. Rev. Lett.* **64**, 677 (1990).

⁷G. Ebert, K. von Klitzing, K. Ploog, and G. Weimann, *J. Phys. C* **16**, 5441 (1983).

⁸M. E. Cage, R. F. Dziuba, B. F. Field, E. R. Williams, S. M. Girvin, A. C. Gossard, D. C. Tsui, and R. J. Wagner, *Phys. Rev. Lett.* **51**, 1374 (1983).

- ⁹P. C. van Son, G. H. Kruihof, and T. M. Klapwijk, *Surf. Sci.* **229**, 57 (1990).
- ¹⁰P. C. van Son and T. M. Klapwijk, *Europhys. Lett.* **12**, 429 (1990).
- ¹¹Ch. Simon, B. B. Goldberg, F. F. Fang, M. K. Thomas, and S. Wright, *Phys. Rev. B* **33**, 1190 (1986); Yu V. Dubrovskii, M. S. Nunuparov, and M. I. Reznikov, *Zh. Eksp. Teor. Fiz.* **94**, 356 (1988) [*Sov. Phys.—JETP* **67**, 632 (1988)].
- ¹²R. G. Mani and J. R. Anderson, *Solid State Commun.* **72**, 949 (1989).
- ¹³F. Kuchar, G. Bauer, G. Weimann, and H. Burkhard, *Surf. Sci.* **142**, 196 (1984).
- ¹⁴S. Komiyama, T. Takamasu, S. Hiyamizu, and S. Sasa, *Solid State Commun.* **54**, 479 (1985); A. V. Gurevich and R. G. Mints, *Pis'ma Zh. Eksp. Teor. Fiz.* **39**, 318 (1984) [*JETP Lett.* **39**, 381 (1984)]; T. Takamasu, S. Komiyama, S. Hiyamizu, and S. Sasa, *Surf. Sci.* **170**, 202 (1986).
- ¹⁵K. Yoshihiro, J. Kinoshita, K. Inagaki, C. Yamanouchi, Y. Murayama, T. Endo, M. Koyanagi, J. Wakabayashi, and S. Kawaji, *Surf. Sci.* **170**, 193 (1986).
- ¹⁶J. R. Kirtley, Z. Schlesinger, T. N. Theis, F. P. Milliken, S. L. Wright, and L. F. Palmateer, *Phys. Rev. B* **34**, 1384 (1986); **34**, 5414 (1986).
- ¹⁷L. Blik, G. Hein, D. Jucknischke, V. Kose, J. Niemeyer, G. Weimann, and W. Schlapp, *Surf. Sci.* **196**, 156 (1988).
- ¹⁸M. D'Iorio, A. S. Sachrajda, D. Landheer, M. Buchanan, T. Moore, C. J. Miner, and A. J. Springthorpe, *Surf. Sci.* **196**, 165 (1988).
- ¹⁹A. S. Sachrajda, D. Landheer, R. Boulet, and T. Moore, *Phys. Rev. B* **39**, 10460 (1989); P. M. Mensz and D. C. Tsui, *ibid.* **40**, 3919 (1989).
- ²⁰P. G. N. de Vegvar, A. M. Chang, G. Timp, P. M. Mankiewich, J. E. Cunningham, R. Behringer, and R. E. Howard, *Phys. Rev. B* **36**, 9366 (1987).
- ²¹P. Streda and K. von Klitzing, *J. Phys. C* **17**, L483 (1984); L. Smrcka, *ibid.* **18**, 2897 (1985).
- ²²D. C. Tsui, G. J. Dolan, and A. C. Gossard, *Bull. Am. Phys. Soc.* **28**, 365 (1983).
- ²³O. Heinonen, P. L. Taylor, and S. M. Girvin, *Phys. Rev. B* **30**, 3016 (1984).
- ²⁴L. Eaves and F. W. Sheard, *Semicond. Sci. Technol.* **1**, 346 (1986).
- ²⁵V. L. Pokrovsky, L. P. Pryadko, and A. L. Talapov, *Zh. Eksp. Teor. Fiz.* **95**, 668 (1989) [*Sov. Phys.—JETP* **68**, 376 (1989)]; *J. Phys.: Condens. Matter* **2**, 1583 (1990).
- ²⁶S. A. Trugman, *Phys. Rev. B* **27**, 7539 (1983).
- ²⁷S. A. Trugman, *Phys. Rev. Lett.* **62**, 579 (1989).
- ²⁸V. G. Mokerov, B. K. Medvedev, V. M. Pudalov, D. A. Rinberg, S. G. Semenchinskii, and Yu. V. Slepnev, *Pis'ma Zh. Eksp. Teor. Fiz.* **47**, 59 (1988) [*JETP Lett.* **47**, 72 (1988)].
- ²⁹M. E. Cage, G. Marullo Reedtz, D. Y. Yu, and C. T. Vandegrift, *Semicond. Sci. Technol.* **5**, 351 (1990).
- ³⁰R. Landauer, *IBM J. Res. Develop.* **1**, 223 (1957); *Z. Phys. B* **68**, 217 (1987).
- ³¹A. D. Stone and A. Szafer, *IBM J. Res. Develop.* **32**, 384 (1988).
- ³²G. H. Kruihof, T. M. Klapwijk, and S. Bakker (unpublished).
- ³³T. Martin and S. Feng, *Phys. Rev. Lett.* **64**, 1971 (1990).